MATERIALS SCIENCE / МАТЕРИАЛОВЕДЕНИЕ

UDC 621.891
DOI 10.17073/0368-0797-2025-3-259-265

Original article
Оригинальная статья

Features of steel contact surface wear in sliding under low contact pressure

M. I. Aleutdinova ✉, **V. V. Fadin**

Institute of Strength Physics and Materials Science, Siberian Branch of the Russian Academy of Sciences (2/4 Akademicheskii Ave., Tomsk 634055, Russian Federation)

✉ aleut@ispms.ru

Abstract. The C235 steel samples were dry-slid along the counterbody (C45 steel) according to the *pin-on-ring* configuration scheme (shaft-pad type) at sliding speeds of 0.75 – 8.0 m/s under a contact pressure of 0.13 MPa. The need for such an experiment is justified by the lack of indicative data on the tribotechnical behavior of steel in sliding contact with steel in the absence of oxidation products in the contact space. Temperature of the sample holder does not exceed 35 °C at all sliding speeds. This allows us to assume that there are no oxidation products on the contact surfaces. Formation of the transfer layer is visually observed in sliding only at low speeds: 0.75 – 1.3 m/s. The friction coefficient decreases during the formation time of the transfer layer and reaches a final value of about 0.4. The sliding surfaces of the samples contain signs of adhesive interaction at all sliding speeds. Adhesion is particularly pronounced on the sliding surface of the sample at a sliding speed of 2.5 m/s. The friction coefficient at this sliding speed has significant fluctuations around 0.8 ± 0.1. At the same time, there is a high rate of wear. Dependence of wear intensity on the sliding speed has maximum at a sliding speed of 2.5 m/s. The lowest wear rate is observed at a sliding speed of 5.0 m/s and at friction coefficient of about 0.7 ± 0.05. A low amplitude of friction coefficient fluctuations (0.7 ± 0.03) is observed when sliding at a speed of 8.0 m/s. *X*-ray phase analysis showed that contact layers of the samples at all sliding speeds have only α-Fe phase with a lattice parameter of about 0.287 nm.

Keywords: sliding metal contact, wear intensity, adhesion, oxidation, friction coefficient, sample holder temperature, phase composition of contact layer

Acknowledgements: The work was carried out within the framework of the state assignment of the Institute of Problems of Socio-Mechanical Problems of the Siberian Branch of the Russian Academy of Sciences, topic No. FWRW-2021-0006.

For citation: Aleutdinova M.I., Fadin V.V. Features of steel contact surface wear in sliding under low contact pressure. *Izvestiya. Ferrous Metallurgy*. 2025;68(3):259–265. https://doi.org/10.17073/0368-0797-2025-3-259-265

Особенности изнашивания контактной поверхности стали при скольжении под низким контактным давлением

М. И. Алеутдинова ✉, **В. В. Фадин**

Институт физики прочности и материаловедения Сибирского отделения РАН (Россия, 634055, Томск, пр. Академический, 2/4)

✉ aleut@ispms.ru

Аннотация. В данной работе сухое скольжение образцов стали Ст3 по контртелу (сталь 45) осуществлялось по схеме сопряжения «*pin-on-ring*» (типа вал–колодка) при скоростях скольжения 0,75 – 8,0 м/с под контактным давлением 0,13 МПа. Необходимость проведения такого эксперимента обоснована отсутствием ориентировочных данных о триботехническом поведении стали в скользящем контакте по стали при отсутствии продуктов окисления в контактном пространстве. Температура держателя образца не превышает 35 °С при всех скоростях скольжения. Это позволяет сделать допущение об отсутствии продуктов окисления на поверхностях контакта. Образование слоя переноса визуально наблюдается при скольжении только с малыми скоростями: 0,75 – 1,3 м/с. Коэффициент трения снижается в течение времени образования слоя переноса и принимает конечное значение около 0,4. Поверхности скольжения образцов содержат признаки адгезионного взаимодействия при всех скоростях скольжения. Особенно отчетливо адгезия наблюдается на поверхности скольжения образца при скорости скольжения 2,5 м/с. Коэффициент трения при этой скорости скольжения имеет значительные колебания около значения 0,8 ± 0,1. Одновременно наблюдается высокая интенсивность изнашивания. Зависимость интенсивности изнашивания от скорости скольжения максимальна при скорости скольжения 2,5 м/с. Самая низкая интенсивность изнашивания наблюдается при скорости скольжения 5,0 м/с и при коэффициенте трения около 0,7 ± 0,05. Низкая амплитуда колебаний коэффициента трения

(0,7 ± 0,03) наблюдается при скольжении со скоростью 8,0 м/с. Рентгеновский фазовый анализ показал, что контактные слои образцов при всех скоростях скольжения имеют только фазу α-Fe с параметром решетки около 0,287 нм.

Ключевые слова: скользящий металлический контакт, интенсивность изнашивания, адгезия, окисление, коэффициент трения, температура держателя образца, фазовый состав контактного слоя

Благодарности: Работа выполнена в рамках государственного задания Института физики прочности и материаловедения Сибирского отделения РАН, тема номер FWRW-2021-0006.

Для цитирования: Алеутдинова М.И., Фадин В.В. Особенности изнашивания контактной поверхности стали при скольжении под низким контактным давлением. *Известия вузов. Черная металлургия*. 2025;68(3):259–265. https://doi.org/10.17073/0368-0797-2025-3-259-265

Introduction

Sliding metal-to-metal contact is typically accompanied by changes in the contact surfaces due to plastic deformation and fatigue failure [1]. The primary measure of this failure is the wear intensity, which serves as the main functional characteristic of the sliding contact. Wear depends on numerous input parameters of the tribosystem, particularly the contact pressure, sliding speed, phase composition of the contact materials, contact geometry, and other factors. These factors determine the wear mechanisms, while wear itself is always driven by adhesive and mechanical interactions of the surface asperities in contact [1; 2]. Wear is also characterized by other output parameters of the tribosystem, such as the friction coefficient, structural parameters of the contact layers, and so on [3 – 6].

One of the most severe types of loading is the effect of dry sliding on metal. In this mode, it is possible to reduce the degradation rate of the contact layer (as well as wear), for example, through self-organization, oxidation on the friction surface, and similar phenomena [3; 5; 7 – 9]. The tribotechnical behavior of friction pairs has been primarily investigated under varying contact pressures and sliding speeds [4; 7; 10 – 16]. It has been noted [7; 10; 15] that the friction coefficient usually decreases with increasing sliding speed, although in some cases, it may increase [16]. Changes in the structure of the contact layers have also been observed, particularly their amorphization and oxidation [4; 8; 13 – 15]. However, the contact temperatures or the sample holder temperatures were not reported, leaving the approximate temperatures that trigger oxidation in the friction zone unknown.

In general, the temperature in the contact zone depends on heat dissipation. Low heat dissipation, caused by the low thermal conductivity of the sample or the design of the sample holder, results in high local temperatures and steep temperature gradients in the contact area. This leads to rapid degradation of the sliding surface under increasing load parameters. Establishing the relationship between wear and the thermal state of the tribosystem is one of the current challenges in tribotechnical materials science. Determining the contact temperature poses certain technical difficulties, as it can only be estimated approximately, whether experimentally or theoretically. In contrast, the sample holder temperature can be determined more easily and accurately, which is why it can serve as one of the characteristics of the sliding contact.

The sliding surface is often ground and cleaned of oxidation products before conducting tribological tests [17 – 19]. Determining the necessity of these actions to reduce wear is of scientific interest. Typically, oxidation products on the contact surface act as a separating medium between the contact surfaces, reducing adhesion, the friction coefficient, and wear [4; 5; 11; 12; 14 – 16; 20]. However, in some cases, an oxidizing gaseous environment causes more severe wear than in an oxygen-free environment [21]. Furthermore, differences in the design of friction assemblies and other tribological parameters across different studies can lead to variations in wear. These differences in friction behavior highlight the need for further research in this area. C235 steel can serve as a model sample, and hardened C45 steel can be used as a model counterbody.

The aim of this study is to investigate the relationship between the wear of C235 steel, the sample holder temperature, and the phase composition of its contact layer during sliding against C45 steel at different sliding speeds.

Materials and methods

To produce work-hardened samples (H_μ = 2.2 GPa) with a cross-sectional area of 2.5×4.0 mm and a height of 6 mm, low-carbon C235 steel (0.2 % C) was used. The phase composition of the contact layers was analyzed using *X*-ray diffraction on a DRON-7 diffractometer with CuK_α radiation. The sliding surfaces were examined using a confocal laser microscope (CLM, Olympus OLS 4100).

Friction loading was applied under a contact pressure P = 0.13 MPa without lubrication, at sliding speeds v = 0.75 ÷ 8.0 m/s, using a CMT-1 tribometer with a *pin-on-ring* configuration shaft-pad type, see Fig. 1). The counterbody was made of C45 steel (0.42 – 0.50 % C) with a hardness of H_μ = 5.8 GPa (53 HRC). Thermocouples (chromel – copel) were attached to the sample holder using screws. The linear wear intensity was calculated

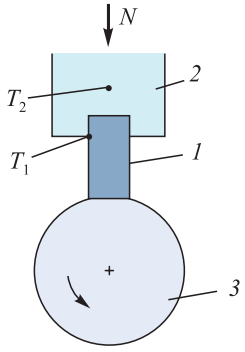

Fig. 1. *Pin-on-ring* configuration diagram:
1 – sample; *2* – sample holder; *3* – counterbody;
T_1 and T_2 – thermocouples on sample holder

Рис. 1. Схема сопряжения *pin-on-ring*:
1 – образец; *2* – держатель образца; *3* – контртело;
T_1 и T_2 – термопары на держателе образца

Values of the obtained parameters

Значения полученных параметров

Parameter	Parameter values at sliding speed, m/s				
	0.75	1.3	2.5	5.0	8.0
a, nm	0.8730	0.2871	0.2873	0.2872	0.2871
I_{110}/I_{200}	4.43	4.83	6.58	11.33	10.32
I_{110}/I_{211}	2.29	2.95	3.15	4.52	3.96
T_1, °C	20	23	28	31	35
T_2, °C	20	21	24	26	28
I_h , μm/km	36	130	250	4	30
B_{110}, deg	0.283	0.330	0.439	0.467	0.485
B_{200}, deg	0.315	0.447	0.471	0.415	0.576

as $I_h = h/D$, where h is the change in sample height per sliding distance D. The friction coefficient was measured using a ZET 7111 strain gauge. Each test was performed three times.

Experimental results and discussion

The obtained parameter values are presented in the Table, where a is the lattice parameter of α-Fe; I_{110}/I_{200} and I_{110}/I_{211} are the intensity ratios of the X-ray diffraction peaks of α-Fe; T_1 and T_2 are the thermocouple temperatures on the sample holder; I_h is the wear intensity; B_{110} and B_{200} are the half- width B_{hkl} of the X-ray peaks.

On the contact surfaces obtained at sliding speeds between 0.75 and 1.3 m/s, there are no clear signs of adhesion (Fig. 2, *a*, *b*). X-ray diffraction analysis of the contact surfaces revealed only the α-Fe phase (Fig. 3, *a*). The lattice parameter of this phase (see Table) is close

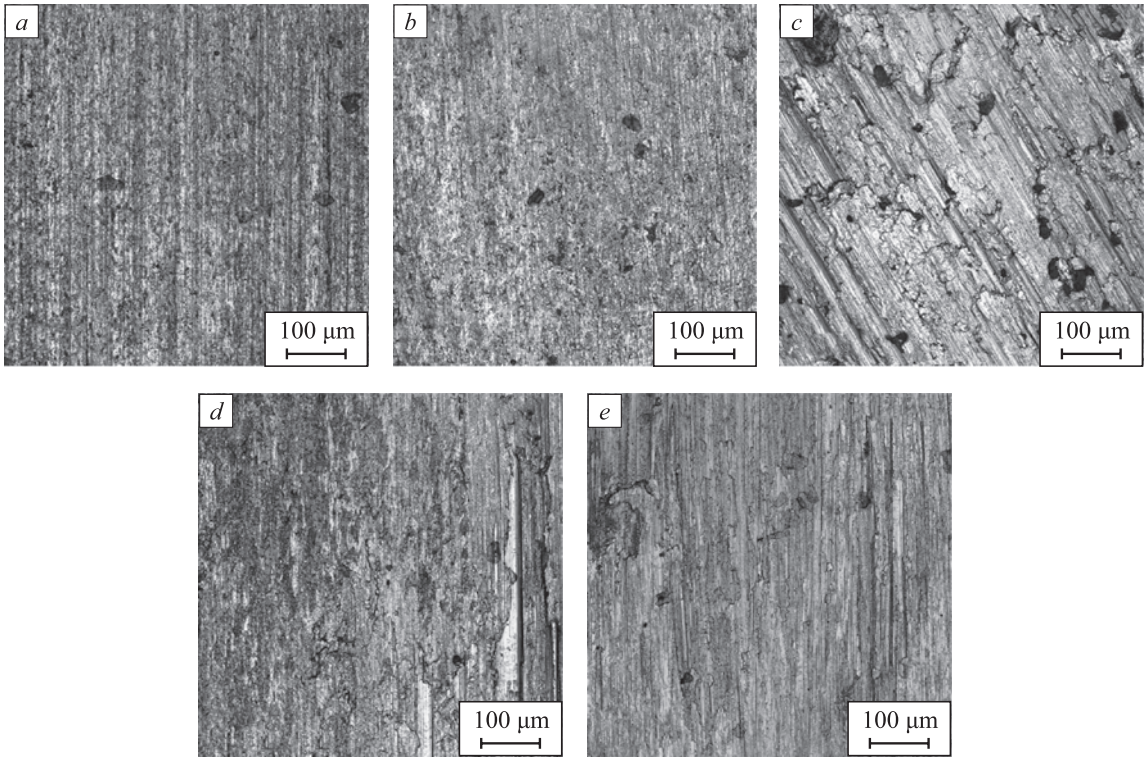

Fig. 2. Confocal images of contact surfaces of the samples (C235 steel) in sliding at speeds of 0.75 (*a*), 1.3 (*b*), 2.5 (*c*), 5.0 (*d*) and 8.0 m/s (*e*)

Рис. 2. Конфокальные изображения поверхностей контакта образцов (сталь Ст3) при скольжении со скоростями 0,75 (*a*), 1,3 (*b*), 2,5 (*c*), 5,0 (*d*) и 8,0 м/с (*e*)

to the standard value of 0.2866 nm (ASTM 6-696 Standard). The friction coefficient f at these speeds decreases over time, stabilizing at approximately 0.4 (Fig. 3, *b*, *c*). This decrease is associated with the formation of a transfer layer on the counterbody surface, which is visually observed and can be easily removed with a cloth. The wear intensity Ih of the samples increases with increasing sliding speed from 0.75 to 1.3 m/s (see Table). The contact surfaces of the samples appear approximately the same (Fig. 2, *a*, *b*).

Increasing the sliding speed to 2.5 m/s results in pronounced signs of strong adhesive interactions on the sample's contact surface (Fig. 2, *c*). Significant fluctuations in the friction coefficient, with high values ranging from 0.7 to 0.8 (Fig. 3, *d*), also indicate strong adhesion at the contact interface. No transfer layer is observed on the counterbody surface. Under these conditions, a high wear intensity I_h is recorded (see Table). The contact layer contains only the α-Fe phase (Fig. 3, *a*), and the lattice parameter remains close to the standard value.

Sliding at a speed of 5.0 m/s occurs without the formation of a transfer layer. There are no visible signs of strong adhesion (Fig. 2, *d*), although adhesion manifests as occasional significant fluctuations in the friction coefficient (Fig. 3, *e*). The contact layer still contains only the α-Fe phase (Fig. 3, *a*). The wear intensity I_h is relatively low (see Table).

Sliding at 8.0 m/s leads to the formation of a surface relief with signs of mild adhesive interaction on the sample's contact surface (Fig. 2, *e*) at a friction coefficient of approximately 0.6. The transfer layer is absent. The contact layer structure consists solely of the α-Fe phase (Fig. 3, *a*), and a high wear intensity I_h is observed (see Table).

The low temperatures T_1 and T_2 of the sample holder (see Table) and the absence of oxidation products on the contact surface (Fig. 3, *a*) indicate a low contact temperature. An increase in the intensity ratios I_{110}/I_{200} and I_{110}/I_{211} of the *X*-ray diffraction peaks is observed with increasing sliding speed (see Table), which may indicate the formation of a deformation-induced texture. At a sliding speed of 8.0 m/s, the intensity ratios begin to decrease, which could be due to partial recrystallization of grains or the removal of the most textured contact sublayer as wear debris. Additionally, there is a general trend of increasing the halfwidth B_{hkl} of the *X*-ray peaks with rising sliding speed (see Table). This is associated with increased residual stresses in the contact layer, a reduction in the size of the coherent scattering regions (CSR), and other factors. Determining the dominant cause of the B_{hkl} increase is beyond the scope of this study.

Repeated mechanical and adhesive interactions that exceed the yield strength in the micro-volumes of surface

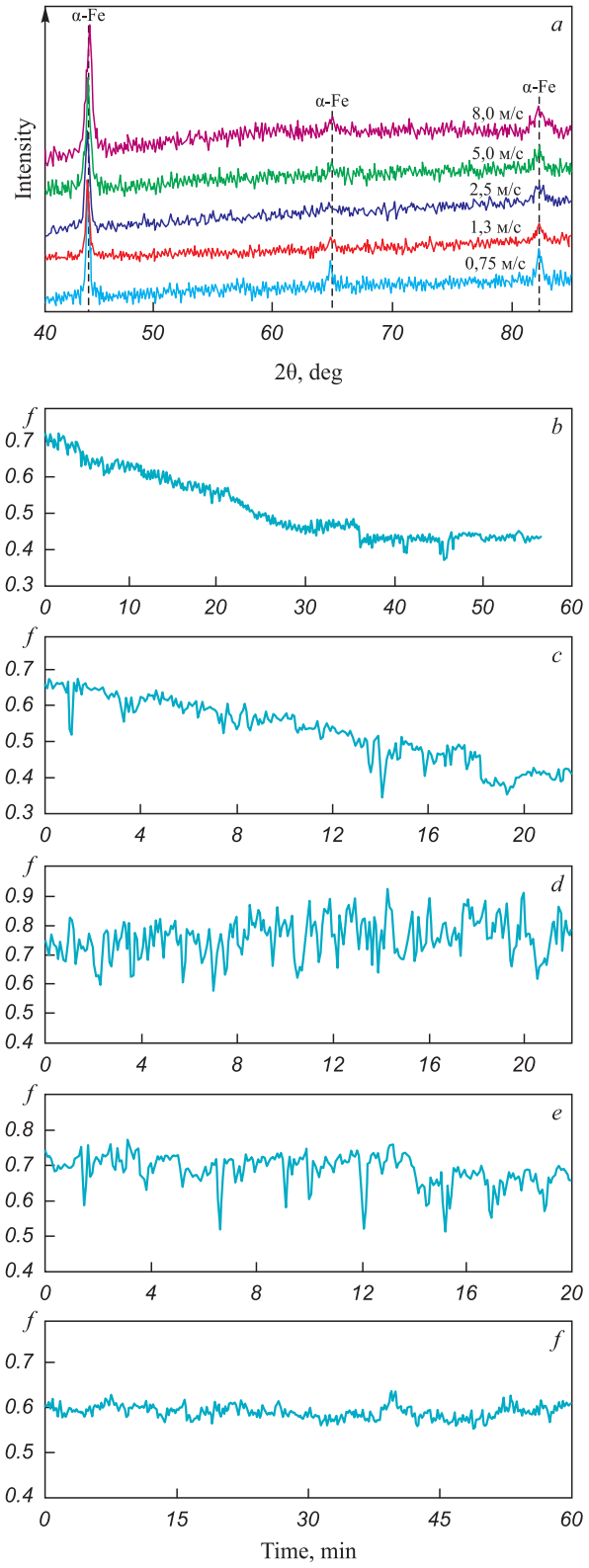

Fig. 3. *X*-ray diffraction patterns of contact surfaces of the samples (C235 steel) when sliding at different speeds (*a*) and time dependence of the friction coefficient in St3/45 steel contact when sliding at a speed of 0.75 (*b*), 1.3 (*c*), 2.5 (*d*), 5.0 (*e*) and 8.0 m/s (*f*)

Рис. 3. Рентгенограммы поверхностей контакта образцов (сталь Ст3) при скольжении с разными скоростями (*a*) и зависимость коэффициента трения от времени в контакте Ст3/сталь 45 при скольжении со скоростью 0,75 (*b*), 1,3 (*c*), 2,5 (*d*), 5,0 (*e*) и 8,0 м/с (*f*)

asperities lead to the accumulation of defects at various scales, resulting in the formation of vacancies, pores, fine grains, and other structural defects in the contact zone. In such cases, fatigue failure occurs, leading to the formation of wear debris. It is worth noting that fatigue-induced failure due to adhesion often dominates over failure caused by the mechanical collision of two opposing microscale asperities [1]. As a rule, the mechanism of contact zone failure depends on the mode of stress relaxation, which, in turn, is determined by the loading conditions. For example, changes in sliding speed – that is, changes in the deformation rate (the rate of energy input into the contact layer) – result in changes in the failure rate of the contact layer (wear intensity I_h; see Table). This indicates a shift in stress relaxation mechanisms with varying sliding speeds v.

At low sliding speeds, mechanical interactions between opposing surface asperities are relatively weak, but prolonged contact within the contact spots promotes sustained adhesive interactions. As a result, adhesion may occur in these contact spots, potentially exceeding the strength of the cohesive bonds beneath the contact area. This can lead to the detachment of micro-volumes from the sample and their transfer to the counterbody surface. The formation of a transfer layer on the counterbody's sliding surface at sliding speeds of 0.75 – 1.3 m/s, along with some sample wear (see Table), aligns with this mechanism. In such cases, asperities may fail either immediately due to adhesion or as a result of fatigue caused by repeated adhesive interactions. This transfer layer is easily removed and contributes to a lower friction coefficient compared to sliding on a clean (initial) contact surface (Fig. 3, *b*, *c*). At these sliding speeds, stress relaxation likely occurs predominantly through plastic shear and the formation of dislocation and disclination structures within a very thin contact layer with weak texture. While these shear mechanisms are active under all friction conditions, they are not always the dominant factors.

High adhesive stresses in the sliding contact can be relaxed only through extensive plastic shear deformation, accompanied by the formation of numerous defects such as micropores, microcracks, and similar imperfections at a sliding speed of 2.5 m/s, that is, when more effective stress relaxation mechanisms are absent.

It is well-established [22; 23], that pulsed loading of metals enhances diffusion, which serves as one of the mechanisms for stress relaxation. This effect is expected to become more pronounced during the impulsive contact of asperities as the sliding speed increases. The low wear observed at v = 5.0 m/s suggests the potential manifestation of this effect, along with the formation of dissipative structures within the contact layer. These structures dissipate once the contact spots disengage. The identification of the specific stress relaxation mechanism lies beyond the scope of this study and will be addressed in future research.

The proposed stress relaxation mechanisms may also be active at v = 8.0 m/s. However, the wear intensity I_h remains relatively high (see Table), as the plastically deformed contact layer tends to expand with increasing sliding speed, accompanied by a rise in the deformation rate. Consequently, an increase in wear is expected at sliding speeds above 5.0 m/s, despite the reduction in the friction coefficient and the amplitude of its fluctuations (Fig. 3, *f*). It is noteworthy that, in many cases, wear intensity I_h decreases with increasing sliding speed [15; 24]. More precise data are anticipated for v > 8.0 m/s in future studies.

Conclusions

This study investigated the wear behavior of C235 steel sliding against C45 steel in the absence of oxidation products between the contact surfaces at sliding speeds up to 8 m/s under a contact pressure of 0.13 MPa.

The contact surfaces consist solely of the α-Fe phase, with a lattice parameter of 0.287 nm across all tested sliding speeds. The sample holder temperature remained below 35 °C throughout the sliding speed range of 0.75 to 8.0 m/s.

Increasing the sliding speed promotes the formation of a pronounced texture within the contact layer. At sliding speeds of 0.75 and 1.3 m/s, a transfer layer is retained on the counterbody surface, leading to a reduction in the friction coefficient to 0.4, accompanied by adhesive wear.

A further increase in the sliding speed to 2.5 m/s results in a significant rise in wear intensity due to strong adhesion at the contact interface. Increasing the sliding speed from 2.5 to 5.0 m/s leads to a sharp decrease in wear intensity, followed by a slight increase in the range of 5.0 – 8.0 m/s.

References / Список литературы

1. Kragelsky I.V., Dobychin M.N., Kombalov V.S. Friction and Wear: Calculation Methods. Elsevier; 2013:474.
2. Bowden F.P., Tabor D. Friction: An Introduction to Tribology. R.E. Krieger Publishing Company; 1982:178.
3. Li B.Y., Li A.C., Zhao S., Meyers M.A. Amorphization by mechanical deformation. *Materials Science and Engineering: R: Reports*. 2022;149:100673. https://doi.org/10.1016/j.mser.2022.100673
4. Wang S.Q., Wang L., Zhao Y.T., Sun Y., Yang Z.R. Mild-to-severe wear transition and transition region of oxidative wear in steels. *Wear*. 2013;306(1-2):311–320. https://doi.org/10.1016/j.wear.2012.08.017
5. Jradi K., Schmitt M., Bistac S. Surface modifications induced by the friction of graphites against steel. *Applied Surface Science*. 2009;255(7):4219–4224.

https://doi.org/10.1016/j.apsusc.2008.11.019

6. Haftlang F., Zarei-Hanzaki A., Abedi H.R. In-situ frictional grain refinement of Ti–29Nb–14Ta–4.5Zr bio-alloy during high-speed sliding wear. *Materials Letters*. 2020;261:127083. https://doi.org/10.1016/j.matlet.2019.127083
7. Nosonovsky M., Bhushan B. Surface self-organization: From wear to self-healing in biological and technical surfaces. *Applied Surface Science*. 2010;256(12):3982–3987. https://doi.org/10.1016/j.apsusc.2010.01.061
8. Yin C.-h., Liang Y.-l., Liang Yu., Li W., Yang M. Formation of a self-lubricating layer by oxidation and solid-state amorphization of nano-lamellar microstructures during dry sliding wear tests. *Acta Materialia*. 2019;166:208–220. https://doi.org/10.1016/j.actamat.2018.12.049
9. Yin C., Qin X., Li Sh., Liang Y., JiangY., Sun H. Amorphization induced by deformation at ferrite-cementite nanointerfaces in a tribolayer and its effect on self-lubricating. *Materials & Design*. 2020;192:108764. https://doi.org/10.1016/j.matdes.2020.108764
10. Kennedy F.E., Lu Y., Baker I., Munroe P.R. The influence of sliding velocity and third bodies on the dry sliding wear of $Fe_{30}Ni_{20}Mn_{25}Al_{25}$ against AISI 347 stainless steel. *Wear*. 2017;374-375:63–76. http://doi.org/10.1016/j.wear.2017.01.002
11. Straffelini G., Pellizzari M., Maines L. Effect of sliding speed and contact pressure on the oxidative wear of austempered ductile iron. *Wear*. 2011;270(9-10):714–719. https://doi.org/10.1016/j.wear.2011.02.004
12. Banerji A., Lukitsch M.J., McClory B., White D.R., Alpas A.T. Effect of iron oxides on sliding friction of thermally sprayed 1010 steel coated cylinder bores. *Wear*. 2017;376-377(A):858–868. https://doi.org/10.1016/j.wear.2017.02.032
13. Zhao H., Feng Yi., Zhou Z., Qian G., Zhang J., Huang X., Zhang X. Effect of electrical current density, apparent contact pressure, and sliding velocity on the electrical sliding wear behavior of Cu–Ti_3AlC_2 composites. *Wear*. 2020;444-445: 203156. https://doi.org/10.1016/j.wear.2019.203156
14. Wang D., Chen Xi., Li F., Chen W., Li H., Yao C. Influence of normal load, electric current and sliding speed on tribological performance of electrical contact interface. *Microelectronics Reliability*. 2023;142:114929. https://doi.org/10.1016/j.microrel.2023.114929
15. Aleutdinova M.I., Fadin V.V. On dry wear of metallic materials in different configurations of sliding electrical contacts against quenched AISI 1045 steel. *Russian Physics Journal*. 2023;65(10):1768–1774. https://doi.org/10.1007/s11182-023-02829-z
16. Threading, Export and Lubrication (Tribology and Tribotechnics). Chichinadze A.V. ed. Moscow: Mashinostroenie; 2003:576. (In Russ.).

    Трение, износ и смазка (трибология и триботехника) / Под общ. ред. А.В. Чичинадзе. Москва: Машиностроение; 2003:576.
17. Khanafi-Benghalem N., Felder E., Loucif K., Montmitonnet P. Plastic deformation of 25CrMo4 steel during wear: Effect of the temperature, the normal force, the sliding velocity and the structural state. *Wear*. 2010;268(1-2):23–40. https://doi.org/10.1016/j.wear.2009.06.036
18. Wang S.Q., Wei M.X., Zhao Y.T. Effects of the tribo-oxide and matrix on dry sliding wear characteristics and mechanisms of a cast steel. *Wear*. 2010;269(5-6):424–434. https://doi.org/10.1016/j.wear.2010.04.028
19. Hu T., Wen C.S., Sun G.Y., Wu S.L., Chu C.L., Wu Z.W., Li G.W., Lu J., Yeung K.W.K., Chu P.K. Wear resistance of NiTi alloy after surface mechanical attrition treatment. *Surface and Coatings Technology*. 2010;205(2):506–510. https://doi.org/10.1016/j.surfcoat.2010.07.023
20. Rynio C., Hattendorf H., Klower J., Eggeler G. On the physical nature of tribolayers and wear debris after sliding wear in a superalloy/steel tribosystem at 25 and 300 °C. *Wear*. 2014;317(1-2):26–38. http://doi.org/10.1016/j.wear.2014.04.022
21. Saravanan Pr., Selyanchyn R., Tanaka Hi., Fujikawa Sh., Lyth S.M., Sugimura J. The effect of oxygen on the tribology of (PEI/GO)15 multilayer solid lubricant coatings on steel substrates. *Wear*. 2019;432-433:102920. https://doi.org/10.1016/j.wear.2019.05.035
22. Larikov L.N., Falochenko V.M., Mazanko V.F. Abnormal acceleration of diffusion during pulse loading of metals. *Reports of the USSR Academy of Sciences*. 1975;221(5): 1073–1075. (In Russ.).

    Лариков Л.Н., Фалоченко В.М., Мазанко В.Ф. Аномальное ускорение диффузии при импульсном нагружении металлов. *Доклады АН СССР*. 1975;221(5):1073–1075.
23. Straumal B.B., Mazikin A.A., Baretzky B., Schütz G., Rabkin E., Valiev R.Z. Accelerated diffusion and phase transformations in CoCu alloys driven by the severe plastic deformation. *Materials Transactions*. 2012;53(1):63–71. https://doi.org/10.2320/matertrans.MD201111
24. Bannaravuri P.K., Birru A.K. Strengthening of mechanical and tribological properties of Al-4.5%Cu matrix alloy with the addition of bamboo leaf ash. *Results in Physics*. 2018; 10:360–373. https://doi.org/10.1016/j.rinp.2018.06.004

Information about the Authors / Сведения об авторах

Marina I. Aleutdinova, *Cand. Sci. (Eng.), Research Associate of the Laboratory of Physics of Surface Hardening*, Institute of Strength Physics and Materials Science, Siberian Branch of Russian Academy of Sciences
ORCID: 0000-0003-4940-9221
E-mail: aleut@ispms.ru

Viktor V. Fadin, *Dr. Sci. (Eng.), Assist. Prof., Senior Researcher of the Laboratory of Physics of Surface Hardening*, Institute of Strength Physics and Materials Science, Siberian Branch of Russian Academy of Sciences
ORCID: 0000-0002-5028-1002
E-mail: fvv@ispms.ru

Марина Ивановна Алеутдинова, *к.т.н., научный сотрудник лаборатории физики упрочнения поверхности*, Институт физики прочности и материаловедения Сибирского отделения РАН
ORCID: 0000-0003-4940-9221
E-mail: aleut@ispms.ru

Виктор Вениаминович Фадин, *д.т.н., доцент, старший научный сотрудник лаборатории физики упрочнения поверхности*, Институт физики прочности и материаловедения Сибирского отделения РАН
ORCID: 0000-0002-5028-1002
E-mail: fvv@ispms.ru

Contribution of the Authors

M. I. Aleutdinova – development of the original project and methodology, conceptualization, calculation of the obtained parameters.
V. V. Fadin – writing and editing the text, conducting research.

Вклад авторов

М. И. Алеутдинова – разработка оригинального проекта и методологии, концептуализация, расчет полученных параметров.
В. В. Фадин – написание и редактирование текста, проведение исследований.

Received 11.10.2024
Revised 24.12.2024
Accepted 26.12.2024

Поступила в редакцию 11.10.2024
После доработки 24.12.2024
Принята к публикации 26.12.2024